Proc. Natl. Acad. Sci. USA
Vol. 96, pp. 6149–6154, May 1999
Biochemistry

Magnesium-dependent folding of self-splicing RNA: Exploring the link between cooperativity, thermodynamics, and kinetics

JIE PAN*, D. THIRUMALAI†§, AND SARAH A. WOODSON*§¶

*Department of Chemistry and Biochemistry, University of Maryland, College Park, MD 20742-2021; and †Institute for Physical Sciences and Technology and Department of Chemistry and Biochemistry, University of Maryland, MD 20742-2431

Communicated by George H. Lorimer, University of Maryland, College Park, MD, March 25, 1999 (received for review December 12, 1998)

ABSTRACT **Folding of the *Tetrahymena* self-splicing RNA into its active conformation involves a set of discrete intermediate states. The Mg^{2+}-dependent equilibrium transition from the intermediates to the native structure is more cooperative than the formation of the intermediates from the unfolded states. We show that the degree of cooperativity is linked to the free energy of each transition and that the rate of the slow transition from the intermediates to the native state decreases exponentially with increasing Mg^{2+} concentration. Monovalent salts, which stabilize the folded RNA nonspecifically, induce states that fold in less than 30 s after Mg^{2+} is added to the RNA. A simple model is proposed that predicts the folding kinetics from the Mg^{2+}-dependent change in the relative stabilities of the intermediate and native states.**

The diverse biological functions performed by RNA molecules in the cell require that they form complex three-dimensional structures (1). A well studied example is the self-splicing intron, or ribozyme, from *Tetrahymena thermophila* rDNA (2). Binding of Mg^{2+} is required to stabilize the folded tertiary structure of the ribozyme and for catalytic activity (3).

Despite recent progress in understanding RNA folding mechanisms (1, 4), the Mg^{2+}-dependent self-assembly of large structures remains a challenging problem. The thermodynamics and kinetics of folding transitions that are coupled to ion binding have been studied in detail for tRNA and other small RNAs (5–9). These studies showed that condensation of the RNA chain is stabilized to a large extent by nonspecific electrostatic screening provided by delocalized, hydrated cations. However, a small number of ions bound in discrete high-affinity sites stabilize specific tertiary conformations (5, 7, 10, 11). This stabilization is accomplished by direct interactions with ligands provided by the folded RNA (12, 13). As a result, binding of Mg^{2+} not only stabilizes the native conformation but also directs the pathway of self-assembly (10, 14).

The complex structure of large RNAs suggests that the folding process is likely to involve multiple equilibrium states. Thermal unfolding of the *Tetrahymena* ribozyme involves at least two transitions (15), and equilibrium and kinetic folding experiments in the presence of $MgCl_2$ revealed intermediates in which only the independently stable P4–P6 domain was folded (16–21). We have shown that urea-induced denaturation of the pre-RNA containing the *Tetrahymena* ribozyme involves at least three states (22), as outlined in Scheme I.

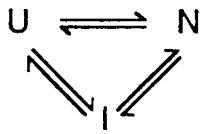

Scheme **I**.

The kinetic partitioning mechanism that we previously proposed (23) postulates that a fraction of the initially unfolded population reaches the native state on the time scale of seconds. This prediction is supported by recent experiments that probed the structure of the ribozyme on second time scales (21). However, the majority of the population reaches the native state N via an intermediate I. Similarly, the equilibrium folding of RNase P RNA, another large catalytic RNA, is best described by a three-state transition, as detected by UV absorbance and CD spectroscopy (24).

Here, we present a simplified framework for considering cooperative transitions in large RNAs and their effect on the Mg^{2+}-dependent folding kinetics. By using the *Tetrahymena* self-splicing RNA as an example, we show that the cooperativity of the Mg^{2+}-dependent I $\Leftrightarrow$ N transition is determined by the relative stabilities of the I and N states at saturating Mg^{2+} concentrations. The intermediate contains at least some nonnative interactions that must dissociate during the transition to the native structure (22, 25). As a result, the increased stability of I at higher Mg^{2+} concentrations leads to a decrease in the rate of folding.

MATERIALS AND METHODS

Preparation of RNA and Native Gel Electrophoresis. Uniformly ^{32}P-labeled *Tetrahymena* precursor RNA (657 nt) was transcribed from plasmid pSW012 as described (26). Pre-RNA was annealed by heating at 95°C for 1 min in splicing buffer without $MgCl_2$ (50 mM Na Hepes/100 mM ammonium sulfate/1 mM EDTA, pH 7.5) followed by rapid cooling ($\leq$30 s) (27) in the presence of 0–10 mM $MgCl_2$ (25). The same procedure was used to anneal samples in the presence of other salts. Glycerol (10% vol/vol) and xylene cyanol (0.1%) were added to samples immediately before loading on a native 6% polyacrylamide gel in 34 mM Tris/66 mM Hepes/0.1 mM EDTA/10 mM $MgCl_2$ (pH 7.5) at 10°C (28). Folding experiments at 30°C were carried out by incubating pre-RNA samples for 2 hr in splicing buffer containing 0–10 mM $MgCl_2$ plus 10% glycerol and xylene cyanol. The fractions of N and I were determined by quantifying bands 1 and 4 relative to the total pre-RNA in each lane by using a PhosphorImager. The data were fit to $f_N = f_\alpha$ or $f_I = 1 - f_\alpha$, with $f_\alpha = (f - f_{min})/(f_{max} - f_{min}) = (C/C_{m\alpha})^n/[1 + (C/C_{m\alpha})^n]$; where C is Mg^{2+} concentration, $C_{m\alpha}$ is the midpoint of the transition, and n is the Hill constant.

Determination of Folding Rates. Pre-RNA was incubated in splicing buffer containing 0–10 mM $MgCl_2$ at 30°C plus 10% (vol/vol) glycerol, as above. Aliquots were removed at specified times up to 120 min and loaded directly into the well of a native 6% polyacrylamide gel as described (22). Unfolding rates were measured by annealing the pre-RNA at 95°C in 6 mM $MgCl_2$ and then diluting into splicing buffer at 30°C so that the final $MgCl_2$ concentration was 2–4.25 mM. The results described

The publication costs of this article were defrayed in part by page charge payment. This article must therefore be hereby marked "*advertisement*" in accordance with 18 U.S.C. §1734 solely to indicate this fact.

PNAS is available online at www.pnas.org.

§To whom reprint requests should be addressed. email: swoodson@jhu.edu or thirum@glue.umd.edu.
¶Present address: Department of Biophysics, Johns Hopkins University, 3400 North Charles Street, Baltimore, MD 21218-2864.

here and elsewhere (29) suggest that folding is arrested when the RNA enters the gel matrix. Folding during the time required for the RNA to enter the gel (15–30 s) was minimized by the low temperatures of the tank buffer (4°C) and gel (<10°C).

The rate equations for the mechanism in Scheme I have been described, and result in two kinetic phases (30). In the limit in which the two phases are well separated, the observed time constants approximate those of the individual pathways. The U-to-N pathway is faster than the smallest accessible times in our experiments, and is ignored in our analysis. The fraction of native or intermediate RNA (f_N or f_I) was quantified as above. The fraction of N (f_N) was fit to $f_N(t) = A_N\,(1 - \exp(-k_N t))$, where A_N is the amplitude of the folding transition. Below 4.5 mM $MgCl_2$, the fraction of I was fit to $f_I(t) = f_I(0) \pm A_I\,(1 - \exp(-k_I t))$, where A_I is the amplitude of the slow transition and $f_I(0)$ is the fraction of I at time zero. The upper sign holds below C_m, and the lower above C_m. Above 4.5 mM $MgCl_2$, f_I was fit to $f_I(t) = f_I(0) + A_{fast}\,(1 - \exp(-k_{fast}t)) + A_I\,(1 - \exp(-k_I t))$, where A_{fast} is the residual amplitude of the fast transition and $k_{fast} \approx 2$–$10\ min^{-1}$. Unfolding reactions were fit to a first-order rate equation.

RESULTS

Magnesium-Dependent Equilibrium Transitions of the Pre-RNA. To describe the role of cations in inducing conformational transitions in RNA, it is necessary to measure the degree of cooperativity in the two equilibrium transitions, namely, U ⇔ I and I ⇔ N. We monitored the fraction of fully folded and partially folded pre-RNA as a function of Mg^{2+} concentration by using nondenaturing PAGE (29). Unrenatured or denatured RNA migrated as a broad smear, suggesting that the initial population is conformationally heterogeneous (24). Much of the RNA secondary structure is expected to be stable under these conditions (15). On incubation in Mg^{2+}-containing buffer or renaturation by heating to 95°C for 1 min and cooling in the presence of $MgCl_2$ (27), the pre-RNA was converted to a mixture of an inactive intermediate (Fig. 1*A*, band 1) and the active or native form (Fig. 1*A*, band 4).

Our earlier work suggested that band 1 of the native gel should be viewed as a collection of conformationally related intermediates (25). Because the number of intermediate states is hard to estimate, we will treat the collection of species in band 1 as a class of nearly equivalent states and denote them as equilibrium intermediate I. Similarly, the ensemble of denatured structures will be considered to be the unfolded state. With these simplifications, the Mg^{2+}-dependent equilibrium folding of the *Tetrahymena* pre-RNA can be described by a three-state model (Scheme I), consistent with previous work (17, 18, 22).

To determine the Mg^{2+} dependence of folding, the pre-RNA was renatured at 95°C in various concentrations of $MgCl_2$ (Fig. 1*B*). At $MgCl_2$ concentrations <2.5 mM, the RNA was distributed between the U and I states. The fraction of I increased only slightly over this range, and a significant amount was formed even when no $MgCl_2$ was added to the sample. As the concentration of $MgCl_2$ was increased to 6 mM, the pre-RNA exhibited a cooperative transition to the native form, with a midpoint (C_m) of 4.1 mM $MgCl_2$. In other experiments, pre-RNA was incubated in buffer containing $MgCl_2$ for 2 hr at 30°C (Fig. 1*C*). The results were qualitatively similar as when the RNA was annealed at high temperatures, although the cooperativity was increased and the midpoint was lower (C_m = 3.4 mM) because of the presence of 10% glycerol in the samples during the incubation period (J.P., unpublished data). In all cases, very similar parameters were obtained from fits to f_N or f_I vs. Mg^{2+} concentration. The maximum extent of folding was ≈80%, presumably because of residual misfolded states.

Cooperativity and Stability Are Linked. The Mg^{2+} dependence of the folding equilibrium (Fig. 1) was used to estimate the stabilities of I and N. The calculation of the free energies of formation of I and N is facilitated by introducing a quantitative measure that describes the extent to which the two equilibrium transitions (U ⇔ I and I ⇔ N) are cooperative. Consider the dimensionless quantity

$$\Omega_c = \frac{C_{max}^2 \left(\frac{df_\alpha}{dC}\right)_{max}}{\Delta C} \qquad [1]$$

where f_α is the population of either I or N, C_{max} is the concentration of Mg^{2+} at which the derivative of f_α with respect to C reaches a maximum, $\left(\frac{df_\alpha}{dC}\right)$ is the value of the derivative at $C = C_{max}$, and ΔC is the width of the curve at 1/2 $\left(\frac{df_\alpha}{dC}\right)$. The value of C_{max} almost always coincides with the midpoint of the transition under consideration. For an infinitely sharp transition, Ω_c tends to infinity, whereas for a noncooperative transition, Ω_c approaches zero.

Because the pre-RNA undergoes a three-state transition, Eq. **1** should be evaluated for the formation of both I and N. If the midpoints for forming I and N are well separated, then the values of Ω_{cI} and Ω_{cN} for the transitions U ⇔ I and I ⇔ N may be calculated independently. The measure of cooperativity in Eq. **1** is dimensionless, and hence one can compare the differences in the cooperativity of formation of I and N on an equal basis. As can be seen in Fig. 1, I ⇔ N is cooperative with respect to Mg^{2+}, and we obtained a value of $\Omega_{cN} = 4.5$ if the pre-RNA was annealed at 95°C or $\Omega_{cN} = 7.6$ when incubated at 30°C.

By contrast, U ⇔ I appeared insensitive to changes in Mg^{2+} concentration. In part, this is because of the fact that some of the RNA reaches the intermediate state during the 15–30 s required for the samples to enter the gel matrix (see below). Because the electrophoresis buffer contained 10 mM $MgCl_2$, this prevented us from accurately determining the amount of I formed as a result of $MgCl_2$ added to the sample. The results of similar experiments with native gels containing 3 mM $MgCl_2$ and the mildly cooperative thermal unfolding of the pre-RNA in 2 mM $MgCl_2$ (J.P., unpublished data) suggest that U ⇔ I is somewhat dependent on Mg^{2+} concentration, but much less cooperative than I ⇔ N.

An estimate of the maximum value of the free energy of forming I and N can be obtained from the values of Ω_{cI} and Ω_{cN}, as follows. By treating the folding process of the pre-RNA as two separate two-state transitions, one can express the fraction of RNA in the I or N states as

$$f_\alpha = 1 - \frac{1}{1 + \exp - \left(\frac{\Delta G_{\beta\alpha} - m_{Mg^{2+}} C}{RT}\right)} \qquad [2]$$

where C is the Mg^{2+} concentration, $\Delta G_{\beta\alpha}$ is the free energy associated with the transition $\beta \Leftrightarrow \alpha$, and $m_{Mg^{2+}}$ gives a measure of the binding of the divalent cation. The linear variation of free energy with C is expected to hold around C_m, the midpoint of the transition. It is clear from Eq. **2** that the transition $\beta \Leftrightarrow \alpha$ occurs over a broad range of Mg^{2+} concentration if $m_{Mg^{2+}}$ is large. Thus, for a highly cooperative transition, we expect $m_{Mg^{2+}}$ to be relatively small. For two-state transitions one can show by substituting Eq. **2** into Eq. **1** that

$$\Omega_{c\alpha} = \tfrac{1}{8}\left(\frac{\Delta G_{\beta\alpha}}{RT}\right)^2 \frac{1}{\ln\,(3 + 2\sqrt{2})} \qquad [3]$$

with α = I or N.

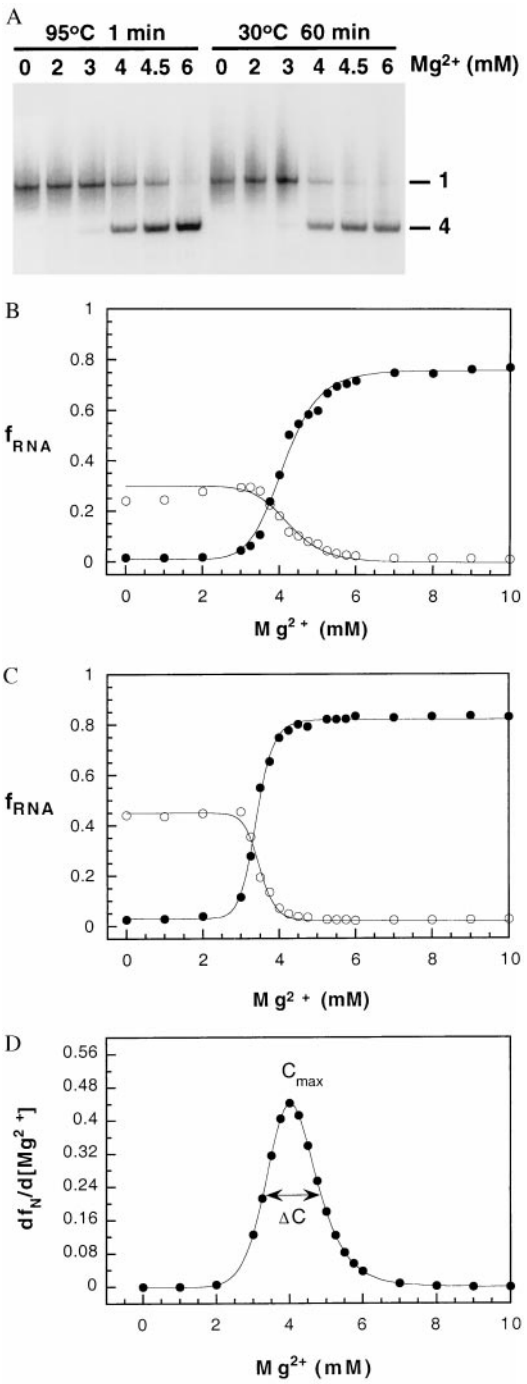

FIG. 1. Magnesium-dependent folding of the *Tetrahymena* pre-RNA. (*A*) ^{32}P-labeled pre-RNA was annealed at 95°C or incubated at 30°C in buffer containing the concentration of $MgCl_2$ indicated above each lane, before loading on a native 6% polyacrylamide gel at 10°C (see *Materials and Methods*). Band 1, folding intermediate (I); band 4, RNA that is competent to self-splice (N) (29). Diffuse radioactivity above and below band 1 is defined as unfolded RNA (U). (*B*) Mg^{2+} dependence of I and N after annealing at 95°C. ●, fraction of native pre-RNA (f_N); ○, fraction of intermediate (f_I). The fraction of unfolded RNA (f_U) is obtained from $f_U + f_I + f_N = 1$. For clarity, f_U is not plotted. f_N and f_I were fit to the Hill equation independently as described in *Materials and Methods*. Values were $C_{m\alpha} = 4.1 \pm 0.03$ and 4.2 ± 0.05 mM, for N and I respectively, and $n = 9.0 \pm 0.8$. **C**, Fraction of I and N after 2 hr at 30°C in splicing buffer plus $MgCl_2$ and 10% glycerol. Symbols and curves are as in *B*. $C_{mN} = 3.4 \pm 0.01$; $C_{mI} = 3.5 \pm 0.02$ mM; $n_N = 15 \pm 0.7$ and $n_I = 17 \pm 1$. (*D*) Derivative of f_N with respect to Mg^{2+} concentration. Values of C_{max} and $(df_x/dC)_{max}$ were obtained analytically from the curve in *B*. ΔC is the width of the curve at $\frac{1}{2}(df_\alpha/dC)_{max}$.

Our measure of cooperativity is qualitatively related to the Hill model. If the Hill constant n is large, then the transition is cooperative, leading to a large value of $\Omega_{c\alpha}$. This implies that the i^{th} Mg^{2+} ion binds more readily than the $(i-1)^{th}$ ion. This feature is captured in Eq. **3** by the linkage between the degree of cooperativity and the free energy gap between the α and β states. The advantage of by using Eqs. **1** and **3** is that we only need to know the properties of the equilibrium curve around the midpoint of the transition, which can be obtained fairly accurately for I ⇔ N. More importantly, a direct estimate of $\Delta G_{\beta\alpha}$ is obtained without making the assumption that the binding constants of all of the Mg^{2+} ions are identical, which is only valid for an infinitely cooperative transition.

From the values of Ω_{cN} above, we find that ΔG_{UN} is −4.8 (95°C annealing) or −6.2 kcal/mol (1 kcal = 4.18 J) (30°C). This establishes that the extent of cooperativity is determined by the relative stability of the initial and final states. The apparently weak dependence of U ⇔ I on Mg^{2+} suggests that ΔG_{UI} is small.

Specificity of Cation Interactions. The decreased cooperativity of U ⇔ I with respect to Mg^{2+} suggested that formation of the intermediate is less dependent on coordination of Mg^{2+} at discrete sites than the native state. If this hypothesis is true, structures resembling I should also result when folding is initiated by monovalent ions. Nonspecific association of monovalent and other divalent ions with the RNA is expected to promote condensation of the RNA, although much greater concentrations of monovalent ions are required to achieve a similar degree of charge stabilization in aqueous solution (31). For example, ≈1 M NaCl is required to stabilize the secondary structure of the *Tetrahymena* ribozyme to the same extent as 5 mM $MgCl_2$ (32).

Folding of the pre-RNA in the presence of Na^+ or NH_4^+ was monitored by gel electrophoresis as before (Fig. 2*A*). When no

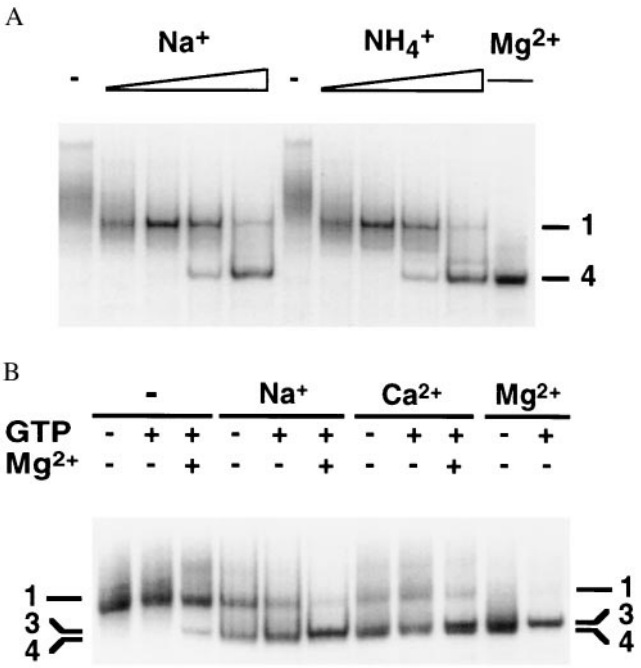

FIG. 2. Monovalent ions induce rapid folding of the pre-RNA. (*A*) RNA was annealed at 95°C in 50 mM Na-Hepes, pH 7.5/1 mM EDTA plus one of the following: no addition (−); 0.1, 0.25, 0.5, or 1 M NaCl; 0.1–1 M $(NH_4)_2SO_4$; or 6 mM $MgCl_2$, before electrophoresis on a native 6% polyacrylamide gel. The gel and running buffer contained 10 mM $MgCl_2$. (*B*) Pre-RNA was annealed as above with no salt (−), 1 M NaCl, 6 mM $CaCl_2$, or 6 mM $MgCl_2$. Samples were incubated for 30 s at 30°C with (+) or without (−) 0.1 mM GTP and 6 mM $MgCl_2$ immediately before loading. The $MgCl_2$ in the gel and running buffer was replaced by 10 mM $CaCl_2$.

$MgCl_2$ was added to the sample, 100–250 mM NaCl was sufficient to induce a band corresponding to the intermediate seen in Fig. 1*A*. Similar results were obtained with $(NH_4)_2SO_4$, indicating that this effect is due primarily to increased ionic strength rather than to specific interactions with Na^+ ions (Fig. 2*A*). Most of the pre-RNA migrated as the fully folded form (band 4) when annealed in 1 M NaCl and no Mg^{2+}. The folded pre-RNA was active, because it was shifted to a band with a slightly lower mobility when incubated with GTP (data not shown). This GTP-dependent electrophoretic species contains a complex of spliced products and is indicative of self-splicing activity (29). We confirmed that self-splicing requires Mg^{2+} or Mn^{2+} under the conditions of these experiments (data not shown). Therefore, the formation of active pre-RNA in these experiments must be because of the presence of Mg^{2+} ions in the electrophoresis buffer.

To further assess the specific requirements for Mg^{2+} during folding, similar experiments were carried out on native gels equilibrated in 10 mM $CaCl_2$. Ca^{2+} stabilizes the tertiary structure of the ribozyme but is not sufficient for catalysis (18, 33). As illustrated in Fig. 2*B*, pre-RNA that was annealed in either 1 M NaCl or 6 mM $CaCl_2$ attained an electrophoretic mobility similar to that of the native state, although band 4 was slightly broadened. In gels containing $CaCl_2$, however, active pre-RNA was only formed if the samples were incubated with 6 mM $MgCl_2$ for 30 s at 30°C before loading. Thus, a fraction of the ion-binding sites must be specifically occupied by Mg^{2+} in the active state, consistent with previous work (33). The minimum number of Mg^{2+} ions bound in the I ⇔ N transition in 100 mM $(NH_4)_2SO_4$ was estimated to be nine, from an analysis of the fraction of native pre-RNA using the Hill equation (Fig. 1*B*). This value is nearly the same as that obtained when the formation of active ribozyme was monitored by photocrosslinking (17, 34).

The results above show that nonspecific cation interactions stabilize the I and N states. Annealing in high concentrations of Na^+ or NH_4^+ or low concentrations of Ca^{2+} induce conformational states that are able to rapidly reach the active state, either during the time required for the RNA to enter the gel matrix (15–30 s) (Fig. 2*A*) or after a 30-s incubation in 6 mM $MgCl_2$ at 30°C (Fig. 2*B*). In early experiments, slower folding of tRNA at low ionic strength was attributed to the prevalence of extended, noncloverleaf secondary structures (6). By analogy, nonspecific ionic interactions may alter the average structure of the unfolded pre-RNA population. The lower gel mobility of I suggests that it is less compact than N, and this is consistent with the fact that greater concentrations of monovalent salts are required to induce formation of N than are required for the formation of I.

Mg^{2+} Dependence of the Folding Kinetics. As the relative stabilities of I and N depend on Mg^{2+}, the folding kinetics of the pre-RNA are also expected to vary with Mg^{2+} concentration. Because the time scale of the direct conversion of U to N is shorter than the time required for samples to enter the native gel (15–30 s), the present experiments only reveal the I ⇔ N transitions, which occur on the minute time scale. Nonetheless, because ≈90% of the RNA population folds via pathways that involve I, many aspects of the folding kinetics can be deduced from the experiments described here. In particular, the rugged energy landscapes arising from topological frustration are manifested in the complex slow kinetics (23).

The populations of I and N were monitored as a function of time (Fig. 3*A*) as described (22) and in *Materials and Methods*. Folding reactions were initiated by adding $MgCl_2$ to unrenatured pre-RNA in 0.1 M $(NH_4)_2SO_4$ at 30°C. Nearly identical results were obtained with pre-RNA that was denatured at 95°C in 7.5 M urea before the start of the folding reaction (data not shown). A significant fraction of I was formed within the initial time of the experiment [f_I (30 s) ≈ 0.2], suggesting that U ⇔ I is rapid for some of the population. This result is consistent with the apparent lack of dependence of f_I on Mg^{2+} concentration in the equilibrium titrations in Fig. 1*B*.

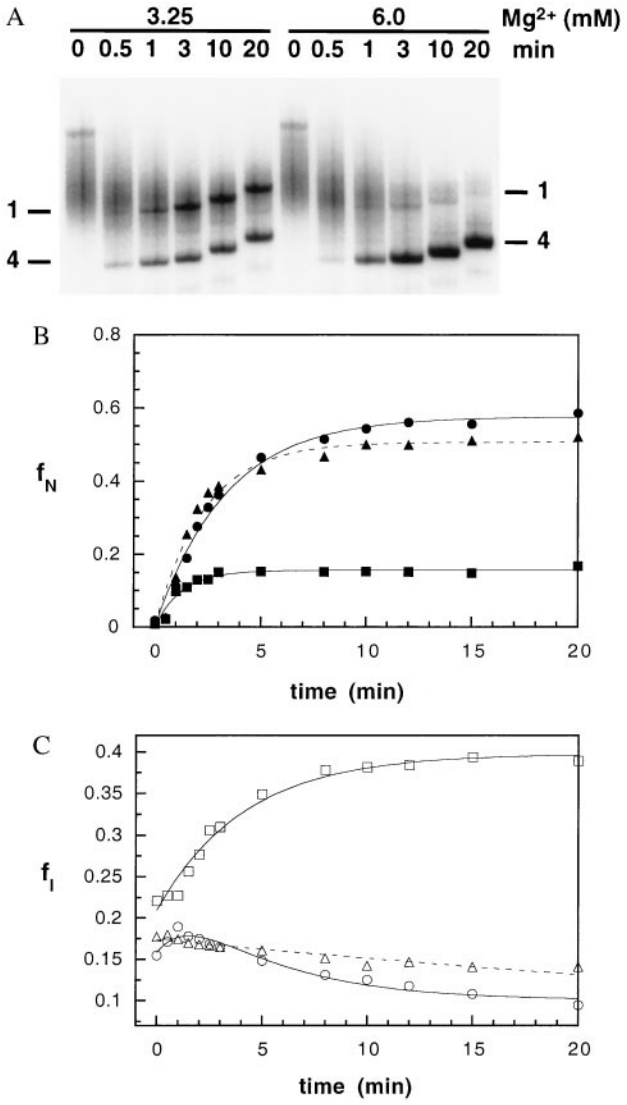

FIG. 3. Folding kinetics of the pre-RNA. (*A*) Folding reactions at 30°C were analyzed after 0–20 min in 3.25 or 6.0 mM $MgCl_2$ by native gel electrophoresis as described (22). The gel was run continuously during the experiment, so that samples loaded at 20 min have migrated a shorter distance. (*B*) Formation of native pre-RNA at 30°C. ■, 3.25 mM; ▲, 4.0 mM; ●, 6.0 mM $MgCl_2$. The data were fit to a first-order rate equation as described in *Materials and Methods*. For clarity, only the first 20 min of the reaction are shown. An additional slow kinetic phase can be resolved when $f_N(t)$ is monitored over 120 min (22). (*C*) Formation of intermediates (I). Symbols are as in *B*. The data were fit to equations with one or two exponential terms (see *Materials and Methods*).

Assuming that rapid formation of I results from nonspecific ion binding, a theoretical estimate of the time scale for U ⇔ I can be made. The nonspecific compaction of chains is predicted to occur on the time scale $\tau_{NC} \approx \tau_0 N^{2.2}$, where N is the number of nucleotides (35). The prefactor, τ_0, which is a function of the viscosity and the persistence length of RNA, is on the order of 1 ns. For the pre-RNA, N = 657, and this yields $\tau_{NC} \approx 2$ ms, which is considerably smaller than the deadtime of our assay. Pan and Sosnick have argued, by using spectroscopic probes, that the equilibrium intermediate in P RNA forms in less than ≈1 ms (24).

A complete analysis of the folding kinetics according to triangle mechanism in Scheme I should include both the fast pathway that is associated with the direct U ⇔ N transition and

the slow pathway involving I. Because the majority of molecules fold via intermediate states, and because I is initially formed rapidly compared with the time required to convert I to N, the appearance of N can be treated as arising from a two-state unimolecular process. With these assumptions, the time dependence of $f_N(t)$ and $f_I(t)$ were fit to single exponential equations (Fig. 3 *B* and *C*). As shown in Fig. 4*A*, the yield of native pre-RNA (A_N) increased cooperatively with Mg^{2+} concentration with a midpoint of 3.7 mM, in agreement with the equilibrium titration experiments (Fig. 1*C*). The yield of the intermediate, however, decreased with increasing Mg^{2+} (Fig. 4*A*). At concentrations of Mg^{2+} below the midpoint of I $\Leftrightarrow$ N, the amount of I continued to increase with time after the first 30 s. Above the midpoint, the fraction of I decreased with time. This change in the direction of the folding process reflects the change in the relative stabilities of I and N.

Rates of unfolding were also measured as a function of Mg^{2+} concentration by diluting renatured pre-RNA into buffer at 30°C containing 2–4.5 mM $MgCl_2$. Little unfolding was observed at Mg^{2+} concentrations above 3.5 mM (data not shown). Below 3.5 mM, however, the rate and extent of unfolding increased rapidly with decreasing Mg^{2+} (k_u = 0.45 min^{-1} at 3.25 mM $MgCl_2$; 0.7 min^{-1} in 3.5 mM $MgCl_2$; $\geq$6 min^{-1} in 2.0 mM $MgCl_2$).

Mg^{2+}-Dependent Stabilities of I and N Determine the Folding Kinetics. An analysis of the rate constant for the folding reaction, k_N, with respect to Mg^{2+} concentration showed that the rate of folding decreased monotonically with increasing Mg^{2+} and became nearly constant when the concentration of the cation was increased beyond 8 mM (Fig. 4*B*). This unexpected result can be rationalized by relating the barrier between I and the most probable transition state with the difference in the free energies of I and N. The simplest model for the variation in ΔG_{IN} is

$$\Delta G_{IN} = \Delta G_{max} + m_{Mg^{2+}}(C_{sat} - C) \quad [4]$$

where C is the concentration of Mg^{2+}, C_{sat} is the saturation value, and ΔG_{max} is the value of ΔG_{IN} at saturating Mg^{2+}. For the pre-RNA considered here, $\Delta G_{max} \approx -4.8$ kcal/mol. The value of the coefficient $m_{Mg^{2+}} = d\Delta G_{IN}/dC$ gives an indication of the number of uncoordinated Mg^{2+} sites and is easily computed from the condition $\Delta G_{IN} = 0$ at C_m. For the pre-RNA, C_m = 4.1 mM, so that $m_{Mg^{2+}} \approx 1$ kcal·mol^{-1}·mM^{-1}.

Alternatively, an estimate of $m_{Mg^{2+}}$ can be made from the dependence of the rate constant k_1 on Mg^{2+} concentration. It follows from the free energy profile describing the unfolding of N to I that the minimum barrier between I and N is $\Delta G^{\ddagger} \geq |\Delta G_{max}| + m_{Mg^{2+}} C$, so that

$$k_1 \leq \exp\left(\frac{-\Delta G_{IN}}{RT}\right) \approx k_0 \exp\left(\frac{-m_{Mg^{2+}}C}{RT}\right) \quad [5]$$

As a result, k_1 should decrease exponentially with increasing concentration of the divalent cation. A semilogarithmic fit to the experimentally determined values of k_1 from 3 to 4.5 mM $MgCl_2$ yielded $m_{Mg^{2+}} \approx 0.5$ kcal·mol^{-1}·mM^{-1} at 30°C (Fig. 4*B*), which is consistent (within a factor of 2) with the estimate from the thermodynamic measurements. Thus, the general outlines of the Mg^{2+}-dependent folding kinetics follow from the thermodynamics of this three-state model.

It is interesting to compare the distinct roles played by Mg^{2+} in the conversion of I to N. We and others have demonstrated that urea accelerates the folding rates of large RNA (22, 24, 36). This result may be understood by supposing that the denaturant does not interact significantly with N but destabilizes the I states (22, 37), leading to the observed increase in rate. In contrast, Mg^{2+} affects both the I and the N states, and the decrease in the folding rate is caused by the effects of the divalent cation on the relative stabilities of N and I. Thus, urea and Mg^{2+} interact very differently with the I states and the native state. These arguments suggest that urea should be most effective under conditions when the concentration of Mg^{2+} is chosen so that N state is more stable than I. In other words, the rate enhancement by urea is greater when $[Mg^{2+}] > C_m$ than when $[Mg^{2+}] < C_m$. This prediction is consistent with the experiments on the *Tetrahymena* ribozyme (38) and RNase P RNA (24), which showed that at a fixed concentration of Mg^{2+} ($>C_m$), the maximum rate of folding was found at the highest urea concentration.

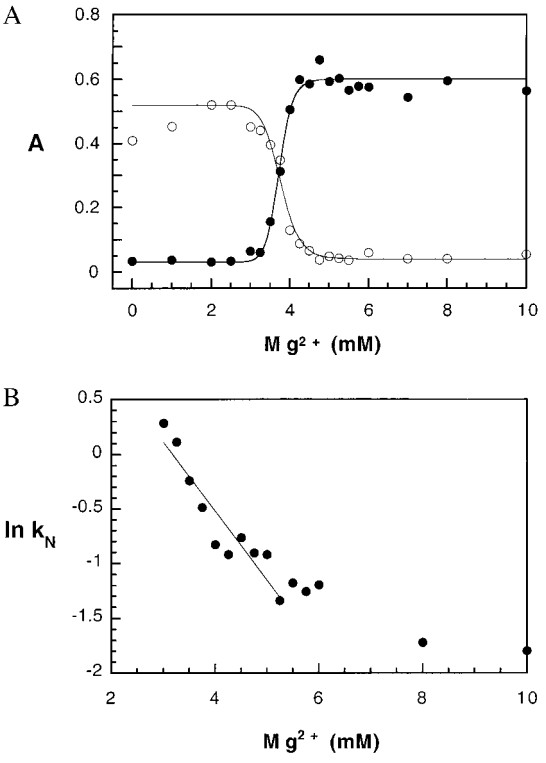

FIG. 4. Mg^{2+} dependence of the folding kinetics. Reactions were carried out in 0 to 10 mM $MgCl_2$ at 30°C as in Fig. 3. (*A*) Amplitude of the folding transitions with increasing $MgCl_2$ concentration. ●, native RNA (A_N); ○, intermediate (A_I). Curves represent the fit to a cooperative binding equation as in Fig. 1*B*, where $f_{N,max} = 0.60$; $f_{N,0} = 0.03$; $K_N = 3.7$; $n_N = 22$; and $f_{I,max} = 0.52$; $f_{I,0} = 0.04$; $K_I = 3.8$; $n_I = 16$. (*B*) Mg^{2+} dependence of observed rate constants (k_N) for I $\Leftrightarrow$ N. The curve represents the best linear fit to ln(k_N) vs. Mg^{2+} concentration, where the slope = $-0.83 = -m_{Mg^{2+}}/RT$.

CONCLUSION

The Mg^{2+}-induced equilibrium transitions to the functional state of the *Tetrahymena* pre-RNA reveal the presence of a stable set of discrete intermediates. We have shown that the transition from I to N is considerably more cooperative than the formation of I from unfolded states, and the degree of cooperativity is found to directly depend on the free energy of the transition. Similar results were obtained by analyzing the data on folding of apomyoglobin after dilution of urea (39), in which it was found that I $\Leftrightarrow$ N was considerably more cooperative than U $\Leftrightarrow$ I (40).

We find that the rate of conversion from I to N decreases monotonically with increasing Mg^{2+} concentration. By contrast, nonspecific ion interactions appear to increase the folding rate of the RNA, presumably by altering the average conformation of the U states. The first result is explained by a model that describes the changes in the underlying energy landscape in terms of the dependence of the relative stabilities of I and N on the concentration of the divalent cation (Fig. 5).

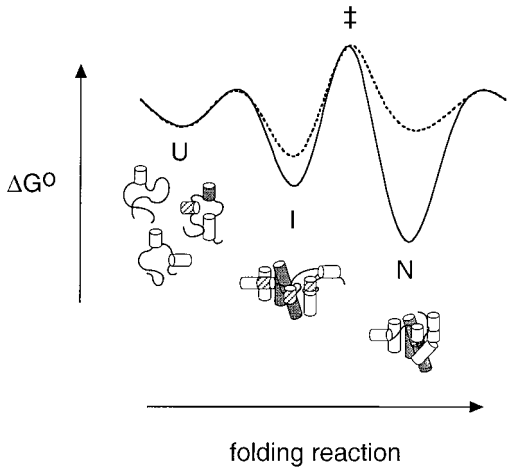

FIG. 5. Three-state model for folding of the *Tetrahymena* pre-RNA. An ensemble of unfolded structures (U) undergo a weakly cooperative and presumably rapid transition to a collection of intermediate states (I) that contain native and nonnative secondary structures (hatched cylinders) (25). I may also be stabilized by tertiary interactions in the P4-P6 domain (dark grey) (36). The transition from I to the native structure (N) is highly cooperative with respect to Mg^{2+}. At Mg^{2+} concentrations above the midpoint ($C > C_m$), N is more stable than I (solid line). When $C < C_m$, N is less stable than I (dashed line). As I is also stabilized somewhat by interactions with Mg^{2+}, the folding rate decreases monotonically with increasing Mg^{2+}. Because this thermodynamic model describes the folding kinetics semi-quantitatively, we expect that the position of the most probable transition state (‡) will vary little with Mg^{2+} concentration.

The dependence of the folding rate on Mg^{2+} can be semi-quantitatively predicted from the parameter $m_{Mg^{2+}}$, which describes the response of I and N to Mg^{2+} concentration. Consistent with this model, we find that the unfolding rate, which corresponds directly to the stability of N, varies slightly more strongly with Mg^{2+} concentration than the rate of folding ($m_{Mg^{2+}} \approx 1.2$). Thus, the relative stabilities of each conformational state not only determine the degree of cooperativity of folding, but also dictate the complex kinetics of the assembly of the native RNA structure.

This work was supported by grants from the National Science Foundation (CHE-96-29845 to D.T.), the National Institutes of Health (GM46686 to S. W.), and a Camille Dreyfus Teacher-Scholar award (to S.W.).

1. Brion, P. & Westhof, E. (1997) *Annu. Rev. Biophys. Biomol. Struct.* **26,** 113–137.
2. Cech, T. R. & Herschlag, D. (1996) in *Nucleic Acids and Molecular Biology*, eds. Eckstein, F. & Lilley, D. M. J. (Springer, Berlin), Vol. 10, pp. 1–17.
3. Pyle, A. M. (1993) *Science* **261,** 709–714.
4. Draper, D. E. (1996) *Nat. Struct. Biol.* **3,** 397–400.
5. Stein, A. & Crothers, D. M. (1976) *Biochemistry* **15,** 157–160.
6. Cole, P. E. & Crothers, D. M. (1972) *Biochemistry* **11,** 4368–4374.
7. Laing, L. G., Gluick, T. C. & Draper, D. E. (1994) *J. Mol. Biol.* **237,** 577–587.
8. Lynch, D. C. & Schimmel, P. R. (1974) *Biochemistry* **13,** 1841–1852.
9. Privalov, P. L. & Filimonov, V. V. (1978) *J. Mol. Biol.* **122,** 447–464.
10. Gluick, T. C., Gerstner, R. B. & Draper, D. E. (1997) *J. Mol. Biol.* **270,** 451–463.
11. Bukhman, Y. V. & Draper, D. E. (1997) *J. Mol. Biol.* **273,** 1020–1031.
12. Cate, J. H., Hanna, R. L. & Doudna, J. A. (1997) *Nat. Struct. Biol.* **4,** 553–558.
13. Correll, C. C., Freeborn, B., Moore, P. B. & Steitz, T. A. (1997) *Cell* **91,** 705–712.
14. Weidner, H. & Crothers, D. M. (1977) *Nucleic Acids Res.* **4,** 3401–3414.
15. Banerjee, A. R., Jaeger, J. A. & Turner, D. H. (1993) *Biochemistry* **32,** 153–163.
16. Banerjee, A. R. & Turner, D. H. (1995) *Biochemistry* **34,** 6504–6512.
17. Downs, W. D. & Cech, T. R. (1996) *RNA* **2,** 718–732.
18. Celander, D. W. & Cech, T. R. (1991) *Science* **251,** 401–407.
19. Zarrinkar, P. P. & Williamson, J. R. (1994) *Science* **265,** 918–924.
20. Zarrinkar, P. P. & Williamson, J. R. (1996) *Nat. Struct. Biol.* **3,** 432–438.
21. Sclavi, B., Sullivan, M., Chance, M. R., Brenowitz, M. & Woodson, S. A. (1998) *Science* **279,** 1940–1943.
22. Pan, J., Thirumalai, D. & Woodson, S. A. (1997) *J. Mol. Biol.* **273,** 7–13.
23. Thirumalai, D. & Woodson, S. A. (1996) *Acc. Chem. Res.* **29,** 433–439.
24. Pan, T. & Sosnick, T. R. (1997) *Nat. Struct. Biol.* **4,** 931–938.
25. Pan, J. & Woodson, S. A. (1998) *J. Mol. Biol.* **280,** 597–609.
26. Emerick, V. L. & Woodson, S. A. (1993) *Biochemistry* **32,** 14062–14067.
27. Walstrum, S. A. & Uhlenbeck, O. C. (1990) *Biochemistry* **29,** 10573–10576.
28. Pyle, A. M., McSwiggen, J. A. & Cech, T. R. (1990) *Proc. Natl. Acad. Sci. USA* **87,** 8187–8191.
29. Emerick, V. L. & Woodson, S. A. (1994) *Proc. Natl. Acad. Sci. USA* **91,** 9675–9679.
30. Szabó, Z. G. (1969) in *Comprehensive Chemical Kinetics*, eds. Bamford, C. H. & Tipper, C. F. H. (Elsevier, Amsterdam), Vol. 2, pp. 1–80.
31. Record, M. T., Zhang, W. T. & Anderson, C. F. (1998) *Adv. Protein Chem.* **51,** 281–353.
32. Jaeger, J. A., Zuker, M. & Turner, D. H. (1990) *Biochemistry* **29,** 10147–10158.
33. Grosshans, C. A. & Cech, T. R. (1989) *Biochemistry* **28,** 6888–6894.
34. Wang, Y. H., Murphy, F. L., Cech, T. R. & Griffith, J. D. (1994) *J. Mol. Biol.* **236,** 64–71.
35. Thirumalai, D. (1995) *J. Phys. I [French]* **5,** 1457–1467.
36. Treiber, D. K., Rook, M. S., Zarrinkar, P. P. & Williamson, J. R. (1998) *Science* **279,** 1943–1946.
37. Camacho, C. J. & Thirumalai, D. (1996) *Protein Sci.* **5,** 1826–1832.
38. Rook, M. S., Treiber, D. K. & Williamson, J. R. (1998) *J. Mol. Biol.* **281,** 609–620.
39. Barrick, D. & Baldwin, R. L. (1993) *Biochemistry* **32,** 3790–3796.
40. Klimov, D. K. & Thirumalai, D. (1998) *Fold. Des.* **3,** 127–139.